Towards a Generic Radiative Transfer Model for the Earth's Surface-Atmosphere System: ESAS-Light

ESTEC Contract No AO/1-5433/07/NL/HE

WP2200:

Preliminary algorithm theoretical basis document for libRadtran demonstration version

Arve Kylling, Claudia Emde and Ulrich Hamann

Deutsches Zentrum für Luft- und Raumfahrt
Wessling, Germany

September 13, 2008

Contents

1 Raman scattering

Air molecules scatter solar radiation. The effects of density, temperature, molecular (re)-orientation, and the role of kinetics, causing elastic and inelastic scattering have primarily an effect on the spectral distribution of the scattered light. These phenomena splits the scattering into several components: (i) an elastic scattering component termed the Gross line, (ii) the Brillouin lines which describe inelastic translational Raman scattering and (iii) inelastic rotational and rotational-vibrational Raman scattering (Young, 1981b; Landgraf et al., 2004). In the Earth's atmosphere the Gross and Brillouin lines may be combined into one elastic scattering component, the so-called Cabannes line. Furthermore, to explain filling in of Fraunhofer lines it suffices to account for Rayleigh scattering and rotational Raman scattering (Kattawar et al., 1981). The classical Rayleigh scattering cross section includes attenuation of energy due to wavelength redistribution by rotational Raman scattering (Young, 1981a). To account for Raman scattering the wavelength redistribution most be accounted for in the emitted energy.

Below a brief summary of Rayleigh and Raman scattering cross sections and phase functions are presented. The derivation of the one-dimensional radiative transfer equation including inelastic rotational Raman scattering may be found in for example Vountas et al. (1998) and will not be repeated here. Rather, the appropriate radiative transfer equation is presented and a discrete ordinate method solution outlined.

1.1 The Raman cross section and phase function

Light scattering in the Earth's atmosphere is caused by scattering of N_2 and O_2 molecules and trace gases. The effect of other gases than N_2 and O_2 on the filling on of spectral lines and absorption lines is minor and will not be included in the discussion below. The cross section for rotational Raman scattering (RRS) by a linear molecule in units of cm^2 is (Chance and Spurr, 1997)

$$\sigma_{RRS}(\lambda_e,\lambda_s) = f_N(T)\gamma^2(\lambda_e)\frac{256\pi^5 C_{J\rightarrow J'}}{27\lambda_s^4}, \tag{1}$$

where λ_e is the wavelength of the incoming radiation and λ_s the wavelength of the scattered radiation. The wavelength shift is calculated from the energy difference between the initial and final state using the relation $E = hc/\lambda$ which gives

$$\lambda_s = \lambda_e + hc(\frac{1}{E_s} - \frac{1}{E_e}) \tag{2}$$

The rotational angular quantum number is denoted by N and J and J' are the total angular momentum for the inital and final states respectively. The total spin momentum quantum number S is the difference between J and N. For nitrogen $S = 0$ and for oxygen $S = 1$.

The polarizability anisotropy for O_2 and N_2 is

$$\gamma_{O_2}(\nu) = 7.149\times10^{-26}\mathrm{cm}^3 + \frac{4.59364\times10^{-15}\mathrm{cm}}{4.82716\times10^{9}\mathrm{cm}^{-2}-\nu^2} \quad (3)$$

$$\gamma_{N_2}(\nu) = -6.01466\times10^{-25}\mathrm{cm}^3 + \frac{2.38557\times10^{-14}\mathrm{cm}}{1.86099\times10^{10}\mathrm{cm}^{-2}-\nu^2} \quad (4)$$

where the wavenumber ν is in cm^{-1}.

The fraction $f_{N,J}(T)$ of molecules in the initial state at temperature T is (Landgraf et al., 2004)

$$f_{N,J}(T) = \frac{g_N}{Z}(2J+1)\exp(-E_J/kT) \quad (5)$$

where E_J is the rotational energy approximated by (Joiner et al., 1995)

$$E_J = J(J+1)hcB_0 \quad (6)$$

where

$$B_0 = 1.4378\mathrm{cm}^{-1}; \qquad O_2. \quad (7)$$

$$B_0 = 1.9897\mathrm{cm}^{-1}; \qquad N_2 \quad (8)$$

The statistical weight factor g_N for nitrogen is $g_N = 6$ and $g_N = 3$ for even and odd J, respectively. For oxygen, $g_N = 0$ and $g_N = 1$ for even and odd J, respectively. From the normalization condition

$$\sum f_{N,J} = 1, \quad (9)$$

the state sum Z for pure rotational Raman scattering is determined. It may be approximated by

$$Z = (2S+1)(2I+1)^2\frac{kT}{2hcB} \quad (10)$$

where the nuclear spin quantum number I is 1 for nitrogen and 0 for oxygen. The electronic spin S is 0 for nitrogen and 1 for oxygen.

Finally the Placzek-Teller coefficients $C_{J\to J'}$ in Eq.1 are for a simple linear molecule ($S = 0$),

$$C_{J\to J+2} = \frac{3(J+1)(J+2)}{2(2J+1)(2J+3)}; \qquad \text{Stokes lines} \quad (11)$$

$$C_{J\to J-2} = \frac{3(J-1)}{2(2J+1)(2J-1)}; \qquad \text{anti-Stokes lines.} \quad (12)$$

These Placzek-Teller coefficients do not apply to molecules with $S = 1$, but will be used for oxygen below.

The Raman phase function is given by (Landgraf et al., 2004; Spurr et al., 2008)

$$P^R(\Phi) = \frac{3}{40}(13+\cos^2\Phi) \quad (13)$$

and the corresponding Legendre expansion coefficient $g_2 = 1/20$.

1.2 The monochromatic radiative transfer equation

The one-dimensional equation for diffuse monochromatic radiation transport at wavelength λ is given by (Chandrasekhar, 1950)

$$\mu\frac{dI(\tau_\lambda,\mu,\Phi)}{d\tau_\lambda} = I(\tau_\lambda,\mu,\Phi) - \frac{\omega_\lambda(\tau_\lambda)}{4\pi}\int_0^{2\pi}d\Phi'\int_{-1}^{1}d\mu' P_\lambda(\tau_\lambda,\mu,\Phi;\mu',\Phi')I(\tau_\lambda,\mu',\Phi') - \frac{\omega_\lambda(\tau_\lambda)I_\lambda^0}{4\pi}P_\lambda(\tau_\lambda,\mu,\Phi;-\mu_0,\Phi_0)e^{-T(\tau_\lambda)}, \quad (14)$$

where $I(\tau_\lambda,\mu,\Phi)$ is the radiance at optical depth τ_λ in direction (μ,Φ), where μ is the cosine of the polar angle and Φ is the polar angle. The solar beam direction is given by $(-\mu_0,\Phi_0)$. Furthermore, $\omega_\lambda(\tau_\lambda)$ is the single scattering albedo and $P_\lambda(\tau_\lambda,\mu,\Phi;\mu',\Phi')$ the phase function describing the likelihood of scattering from incident direction (μ',Φ') into the scattering direction (μ,Φ). The incident flux is given by $\mu_0 I_\lambda^0$ and $e^{-T(\tau_\lambda)}$ is the beam transmittance for a slant optical thickness $T(\tau_\lambda)$. For the plane-parallel case $T(\tau_\lambda)=\tau/\mu_0$. It is for this case that the DISORT (Stamnes et al., 1988) routine solves Eq. 14. For the pseudospherical case the transmittance is described by the Chapman function *ch*: $T(\tau_\lambda)=ch(\tau,\mu_0)$ (Dahlback and Stamnes, 1991). This version of Eq. 14 is solved by sdisort.

1.3 The radiative transfer equation including Raman scattering

The radiative transfer equation including rotational Raman scattering has been derived by several authors (Landgraf et al., 2004; Vountas et al., 1998). Treating rotational Raman scattering as a first-order perturbation the radiative transfer equation becomes (Spurr et al., 2008)

$$\begin{aligned}\mu\frac{dI(\tau_\lambda,\mu,\Phi)}{d\tau_\lambda} = {} & I(\tau_\lambda,\mu,\Phi) - \frac{\omega_\lambda^C(\tau_\lambda)}{4\pi}\int_0^{2\pi}d\Phi'\int_{-1}^{1}d\mu' P_\lambda^C(\tau_\lambda,\mu,\Phi;\mu',\Phi')I(\tau_\lambda,\mu',\Phi') \\ & - \frac{\omega_\lambda^C(\tau_\lambda)I_\lambda^0}{4\pi}P_\lambda^C(\tau_\lambda,\mu,\Phi;-\mu_0',\Phi_0')e^{-T(\tau_\lambda)} \\ & - \sum_{s=1}^{NS}\frac{\omega_{\lambda_s}^R(\tau_{\lambda_s})}{4\pi}\int_0^{2\pi}d\Phi'\int_{-1}^{1}d\mu' P_{\lambda_s}^R(\tau_{\lambda_s},\mu,\Phi;\mu',\Phi')I(\tau_{\lambda_s},\mu',\Phi') \\ & - \sum_{s=1}^{NS}\frac{\omega_{\lambda_s}^R(\tau_{\lambda_s})I_{\lambda_s}^0}{4\pi}P_{\lambda_s}^R(\tau_{\lambda_s},\mu,\Phi;-\mu_0',\Phi_0')e^{-T(\tau_{\lambda_s})}. \quad (15)\end{aligned}$$

Here the single scattering albedo for elastic scattering and the corresponding phase function is denoted by $\omega_\lambda^C(\tau_\lambda)$ and $P_\lambda^C(\tau_\lambda,\mu,\Phi;\mu',\Phi')$, respectively, and is the contribution from molecular Cabannes scattering. The Raman gain single scattering albedo is $\omega_{\lambda_s}^R(\tau_{\lambda_s})$ and the Raman phase function $P_{\lambda_s}^R(\tau_{\lambda_s},\mu,\Phi;\mu',\Phi')$ while τ_{λ_s} is the optical depth at the Raman shifted wavelength λ_s. The two last terms in Eq. 15 represents Raman inelastically scattered light from Raman-shifted wavelengths.

Using the following relationship

$$\omega_\lambda^E(\tau_\lambda)P_\lambda^E(\tau_\lambda,\mu,\Phi;-\mu',\Phi') = \omega_\lambda^C(\tau_\lambda)P_\lambda^C(\tau_\lambda,\mu,\Phi;-\mu',\Phi') + \omega_\lambda^{RL}(\tau_\lambda)P_\lambda^R L(\tau_\lambda,\mu,\Phi;-\mu',\Phi') \quad (16)$$

Eq. 15 may be rewritten according to Spurr et al. (2008) as:

$$\begin{aligned}\mu\frac{dI(\tau_\lambda,\mu,\Phi)}{d\tau_\lambda} &= I(\tau_\lambda,\mu,\Phi)-\frac{\omega^E_\lambda(\tau_\lambda)}{4\pi}\int_0^{2\pi}d\Phi'\int_{-1}^{1}d\mu' P^E_\lambda(\tau_\lambda,\mu,\Phi;\mu',\Phi')I(\tau_\lambda,\mu',\Phi')\\ &-\frac{\omega^E_\lambda(\tau_\lambda)I^0_\lambda}{4\pi}P^E_\lambda(\tau_\lambda,\mu,\Phi;-\mu'_0,\Phi'_0)e^{-T(\tau_\lambda)}\\ &+\frac{\omega^{RL}_\lambda(\tau_\lambda)}{4\pi}\int_0^{2\pi}d\Phi'\int_{-1}^{1}d\mu' P^R_\lambda(\tau_\lambda,\mu,\Phi;\mu',\Phi')I(\tau_\lambda,\mu',\Phi')\\ &+\frac{\omega^{RL}_\lambda(\tau_\lambda)I^0_\lambda}{4\pi}P^R_\lambda(\tau_\lambda,\mu,\Phi;-\mu'_0,\Phi'_0)e^{-T(\tau_\lambda)}\\ &-\sum_{s=1}^{NS}\frac{\omega^R_{\lambda_s}(\tau_{\lambda_s})}{4\pi}\int_0^{2\pi}d\Phi'\int_{-1}^{1}d\mu' P^R_{\lambda_s}(\tau_{\lambda_s},\mu,\Phi;\mu',\Phi')I(\tau_{\lambda_s},\mu',\Phi')\\ &-\sum_{s=1}^{NS}\frac{\omega^R_{\lambda_s}(\tau_{\lambda_s})I^0_{\lambda_s}}{4\pi}P^R_{\lambda_s}(\tau_{\lambda_s},\mu,\Phi;-\mu'_0,\Phi'_0)e^{-T(\tau_{\lambda_s})}. \qquad (17)\end{aligned}$$

1.3.1 The radiative transfer equation for first-order Raman scattering

In the first-order Raman scattering approximation the undisturbed zeroth order or elastic scattering only, Eq. 14, is solved first. This gives the elastic radiance $I^E(\tau_\lambda,\mu,\Phi)$ which is inserted into the 4th and 6th terms on the right side of Eq. 17 to yield:

$$\begin{aligned}\mu\frac{dI(\tau_\lambda,\mu,\Phi)}{d\tau_\lambda} &= I(\tau_\lambda,\mu,\Phi)-\frac{\omega^E_\lambda(\tau_\lambda)}{4\pi}\int_0^{2\pi}d\Phi'\int_{-1}^{1}d\mu' P^E_\lambda(\tau_\lambda,\mu,\Phi;\mu',\Phi')I(\tau_\lambda,\mu',\Phi')\\ &-\frac{\omega^E_\lambda(\tau_\lambda)I^0_\lambda}{4\pi}P^E_\lambda(\tau_\lambda,\mu,\Phi;-\mu'_0,\Phi'_0)e^{-T(\tau_\lambda)}\\ &+\frac{\omega^{RL}_\lambda(\tau_\lambda)}{4\pi}\int_0^{2\pi}d\Phi'\int_{-1}^{1}d\mu' P^R_\lambda(\tau_\lambda,\mu,\Phi;\mu',\Phi')I^E(\tau_\lambda,\mu',\Phi')\\ &+\frac{\omega^{RL}_\lambda(\tau_\lambda)I^0_\lambda}{4\pi}P^R_\lambda(\tau_\lambda,\mu,\Phi;-\mu'_0,\Phi'_0)e^{-T(\tau_\lambda)}\\ &-\sum_{s=1}^{NS}\frac{\omega^R_{\lambda_s}(\tau_{\lambda_s})}{4\pi}\int_0^{2\pi}d\Phi'\int_{-1}^{1}d\mu' P^R_{\lambda_s}(\tau_{\lambda_s},\mu,\Phi;\mu',\Phi')I^E(\tau_{\lambda_s},\mu',\Phi')\\ &-\sum_{s=1}^{NS}\frac{\omega^R_{\lambda_s}(\tau_{\lambda_s})I^0_{\lambda_s}}{4\pi}P^R_{\lambda_s}(\tau_{\lambda_s},\mu,\Phi;-\mu'_0,\Phi'_0)e^{-T(\tau_{\lambda_s})}. \qquad (18)\end{aligned}$$

Eq. 18 may be rewritten

$$\begin{aligned}\mu\frac{dI(\tau_\lambda,\mu,\Phi)}{d\tau_\lambda} &= I(\tau_\lambda,\mu,\Phi)-\frac{\omega^E_\lambda(\tau_\lambda)}{4\pi}\int_0^{2\pi}d\Phi'\int_{-1}^{1}d\mu' P^E_\lambda(\tau_\lambda,\mu,\Phi;\mu',\Phi')I(\tau_\lambda,\mu',\Phi')\\ &-\frac{\omega^E_\lambda(\tau_\lambda)I^0_\lambda}{4\pi}P^E_\lambda(\tau_\lambda,\mu,\Phi;-\mu'_0,\Phi'_0)e^{-T(\tau_\lambda)}\\ &-Q(\tau_\lambda,\mu,\Phi), \qquad (19)\end{aligned}$$

where the source term

$$\begin{aligned} Q(\tau_\lambda,\mu,\Phi) &= +\sum_{s=1}^{NS}\frac{\omega^R_{\lambda_s}(\tau_{\lambda_s})}{4\pi}\int_0^{2\pi}d\Phi'\int_{-1}^{1}d\mu' P^R_{\lambda_s}(\tau_{\lambda_s},\mu,\Phi;\mu',\Phi')I^E(\tau_{\lambda_s},\mu',\Phi') \\ &\quad +\sum_{s=1}^{NS}\frac{\omega^R_{\lambda_s}(\tau_{\lambda_s})I^0_{\lambda_s}}{4\pi}P^R_{\lambda_s}(\tau_{\lambda_s},\mu,\Phi;-\mu'_0,\Phi'_0)e^{-T(\tau_{\lambda_s})} \\ &\quad -\frac{\omega^{RL}_\lambda(\tau_\lambda)}{4\pi}\int_0^{2\pi}d\Phi'\int_{-1}^{1}d\mu' P^R_\lambda(\tau_\lambda,\mu,\Phi;\mu',\Phi')I^E(\tau_\lambda,\mu',\Phi') \\ &\quad -\frac{\omega^{RL}_\lambda(\tau_\lambda)I^0_\lambda}{4\pi}P^R_\lambda(\tau_\lambda,\mu,\Phi;-\mu'_0,\Phi'_0)e^{-T(\tau_\lambda)}. \end{aligned} \tag{20}$$

1.3.2 A discrete ordinate method solution

In the discrete ordinate method the azimuth dependence is separated by expanding the radiance as a Fourier cosine series (Chandrasekhar, 1950, p. 149-150):

$$I(\tau_\lambda,\mu,\Phi)=\sum_{m=0}^{2M-1}I(\tau_\lambda,\pm\mu)\cos m(\Phi_0-\Phi). \tag{21}$$

Furthermore the phase function is written in terms of Legendre polynomials:

$$P(\tau,\mu,\Phi;\mu',\Phi')=P(\tau,\cos\Theta)=\sum_{l=0}^{2M-1}(2l+1)g_l(\tau)P_l(\cos\Theta), \tag{22}$$

where the expansion coefficients are given by

$$g_l(\tau)=\frac{1}{2}\int_{-1}^{1}P_l(\cos\Theta)P(\tau,\cos\Theta)d\cos\Theta. \tag{23}$$

Using the relation

$$\cos\Theta=-\mu'\mu+\sqrt{1-\mu'^2}\sqrt{1-\mu^2}\cos(\Phi-\Phi'), \tag{24}$$

and applying the addition theorem for spherical harmonics (see Jackson (1975, p. 100-102) for a proof of the addition theorem for spherical harmonics) to Eq. 22 the following expression is obtained for the phase function:

$$\begin{aligned} P(\tau,\mu,\Phi;\mu',\Phi') &= P(\tau,\cos\Theta) \\ &= \sum_{l=0}^{2M-1}(2l+1)g_l(\tau)\Big\{P_l(\mu)P_l(\mu')+2\sum_{m=1}^{l}\Lambda^m_l(\mu)\Lambda^m_l(\mu')\cos m(\phi-\phi')\Big\} \\ &= \sum_{m=0}^{2M-1}(2-\delta_{0,m})\Big\{\sum_{l=m}^{2M-1}(2l+1)g_l(\tau)\Lambda^m_l(\mu)\Lambda^m_l(\mu')\Big\}\cos m(\phi-\phi') \end{aligned} \tag{25}$$

where the order of summation has been changed between the two last lines and $\Lambda_l^m(\mu)$ is the normalized associated Legendre polynomial which are preferred instead of the associated Legendre polynomials for numerical reasons (Stamnes et al., 2000, section 3.3.2).

Insertion of Eqs. 21 and 25 into Eq. 19, performing the integrals over Φ' gives for each Fourier component the following equation:

$$\begin{aligned}\mu\frac{dI^m(\tau_\lambda,\mu)}{d\tau_\lambda} &= I^m(\tau_\lambda,\mu)-\frac{\omega_\lambda^E(\tau_\lambda)}{2}\int_{-1}^{1}d\mu'\Pi_d^E(\tau_{\lambda_s},\mu,\mu')I^m(\tau_\lambda,\mu')\\ &\quad -\frac{\omega_\lambda^E(\tau_\lambda)I_\lambda^0}{4\pi}(2-\delta_{0,m})\Pi_b^E(\tau_{\lambda_s},\mu,\mu')e^{-T(\tau_\lambda)}\\ &\quad -Q^m(\tau_\lambda,\mu),\end{aligned} \tag{26}$$

where the source term

$$\begin{aligned}Q^m(\tau_\lambda,\mu) = &+\sum_{s=1}^{NS}\frac{\omega_{\lambda_s}^R(\tau_{\lambda_s})}{2}\int_{-1}^{1}d\mu'\Pi_d^R(\tau_{\lambda_s},\mu,\mu')I^{E,m}(\tau_{\lambda_s},\mu')\\ &+\sum_{s=1}^{NS}\frac{\omega_{\lambda_s}^R(\tau_{\lambda_s})I_{\lambda_s}^0}{4\pi}(2-\delta_{0,m})\Pi_b^R(\tau_{\lambda_s},\mu,\mu_0)e^{-T(\tau_{\lambda_s})}\\ &-\frac{\omega_\lambda^{RL}(\tau_\lambda)}{2}\int_{-1}^{1}d\mu'\Pi_d^R(\tau_\lambda,\mu,\mu')I^{E,m}(\tau_\lambda,\mu')\\ &-\frac{\omega_\lambda^{RL}(\tau_\lambda)I_\lambda^0}{4\pi}(2-\delta_{0,m})\Pi_b^R(\tau_\lambda,\mu,\mu_0)e^{-T(\tau_\lambda)}.\end{aligned} \tag{27}$$

and

$$\Pi_b^x(\tau,\mu,\mu') = \sum_{l=m}^{2M-1}(2l+1)g_l^x(\tau)(-1)^{l+m}\Lambda_l^m(\mu)\Lambda_l^m(\mu_0) \tag{28}$$

$$\Pi_d^x(\tau,\mu,\mu') = \sum_{l=m}^{2M-1}(2l+1)g_l^x(\tau_{\lambda_s})\Lambda_l^m(\mu)\Lambda_l^m(\mu'), \tag{29}$$

where $x=E,R$. It is noted that for $x=R$ only terms for $m=0,1,2$ contribute in the above sums, see Raman phase function Eq. 13.

By replacing the integrals in Eq. 26 by a sum using double Gaussian quadrature the discrete

ordinate solution is obtained (Chandrasekhar, 1950; Stamnes et al., 1988):

$$\begin{aligned}
\mu_i \frac{dI^m(\tau_\lambda,\mu_i)}{d\tau_\lambda} &= I^m(\tau_\lambda,\mu_i) - \frac{\omega_\lambda^E(\tau_\lambda)}{2} \sum_{\substack{j=-1 \\ j\neq 0}}^{j=1} c_j \Pi_d^E(\tau_{\lambda_s},\mu_i,\mu_j) I^m(\tau_\lambda,\mu_j) \\
&\quad - \frac{\omega_\lambda^E(\tau_\lambda) I_\lambda^0}{4\pi}(2-\delta_{0,m})\Pi_b^E(\tau_{\lambda_s},\mu_i,\mu_0) e^{-T(\tau_\lambda)} \\
&\quad - Q^m(\tau_\lambda,\mu_i), \qquad (30)
\end{aligned}$$

$$\begin{aligned}
Q^m(\tau_\lambda,\mu_i) = &+ \sum_{s=1}^{NS} \frac{\omega_{\lambda_s}^R(\tau_{\lambda_s})}{2} \sum_{\substack{j=-1 \\ j\neq 0}}^{j=1} c_j \Pi_d^R(\tau_{\lambda_s},\mu_i,\mu_j) I^{E,m}(\tau_{\lambda_s},\mu_i) \\
&+ \sum_{s=1}^{NS} \frac{\omega_{\lambda_s}^R(\tau_{\lambda_s}) I_{\lambda_s}^0}{4\pi}(2-\delta_{0,m})\Pi_b^R(\tau_{\lambda_s},\mu_i,\mu_0) e^{-T(\tau_{\lambda_s})} \\
&- \frac{\omega_\lambda^{RL}(\tau_\lambda)}{2} \sum_{\substack{j=-1 \\ j\neq 0}}^{j=1} c_j \Pi_d^R(\tau_\lambda,\mu_i,\mu_j) I^{E,m}(\tau_\lambda,\mu_j) \\
&- \frac{\omega_\lambda^{RL}(\tau_\lambda) I_\lambda^0}{4\pi}(2-\delta_{0,m})\Pi_b^R(\tau_\lambda,\mu_i,\mu_0) e^{-T(\tau_\lambda)}, \qquad (31)
\end{aligned}$$

where μ_i and c_i are quadrature angles and weights respectively.

Eqs. 30-31 are a system of $2N$ coupled differential equations for which analytic solutions do not exist. A solution of an equation similar to Eq. 30, but with a general source term instead of direct beam source term and the Raman scattering source terms, has been given by Kylling and Stamnes (1992). The qdisort solver included in libRadtran, is an implementation of this solution procedure. In addition to the particular solution for the general source term it also includes particular solutions for the direct beam source and optionally a thermal source. The solution of the transport equation for a general source term is given in Kylling and Stamnes (1992) and will not be repeated here.

2 Polarized radiative transfer

Observations of polarized radiance may provide much more detailed information about atmospheric constituents than unpolarized measurements, in particular about aerosol particles. However, polarization of atmospheric radiation is neglected by most radiative transfer models, although even the error in the unpolarized radiance may amount to 10%. The solver polradtran (Evans and Stephens, 1991) that computes polarized radiances for 1D plane-parallel atmospheres is already available in libRadtran.

The Monte Carlo solver MYSTIC (Mayer, 2000; Emde and Mayer, 2007) which so far calculates scalar radiative transfer in 3D complex media will be extended to solve the vector radiative transfer equation. There are several major differences between scalar and vector radiative transfer. One major difference is that the calculation requires a 4x4 phase matrix instead of a phase function, a 4x4 extinction matrix instead of an extinction coefficient and an absorption vector instead of an absorption coefficient.

The Rayleigh phase matrix is well known. Liquid water cloud droplets are nearly spherical so that Mie theory can be used to calculate the phase matrix. Ice clouds particles are hexagonal. In this case the geometrical optics method can be used to generate the optical properties if the wavelength of the radiation is much smaller than the particle size (solar radiation). Aerosols swell if the relative humidity is large enough, and one can assume nearly spherical shapes, so that Mie theory can be used. For aspherical aerosols the T-matrix method may be applied to calculate optical properties.

This chapter deals with the theoretical background for polarized radiative transfer. Part of it has been adapted from Emde (2005) which is based on the book by Mishchenko et al. (2002). This document is not meant to be a description of the Monte Carlo solver, it should provide the theoretical background needed to implement polarization. The implementation of polarization in the MYSTIC Monte Carlo solver is described in the development plan (Emde and Kylling, 2008, WP2300 report).

2.1 Definition of the Stokes parameters

Sensors usually do not measure directly the electric and the magnetic fields associated with a beam of radiation. They measure quantities that are time averages of real-valued linear combinations of products of field vector components and have the dimension of intensity. Examples of such observable quantities are the Stokes parameters. Fig. 1 shows the coordinate system used to describe the direction of propagation $\hat{\mathbf{n}}$ and the polarization state of a plane electromagnetic wave.

The unit vector $\hat{\mathbf{n}}$ can equivalently be described by a couplet (θ, ϕ), where $\theta \in [0, \pi]$ is the polar (zenith) angle and $\phi \in [0, 2\pi)$ is the azimuth angle. The electric field at the observation point is given by $\mathbf{E} = \mathbf{E}_\theta + \mathbf{E}_\phi$, where $\mathbf{E}_\theta$ and $\mathbf{E}_\phi$ are the θ- and ϕ- components of the electric field vector. $\mathbf{E}_\theta$ lies in the meridional plane, which is the plane through $\hat{\mathbf{n}}$ and the z-axis, and $\mathbf{E}_\phi$ is perpendicular to this plane.

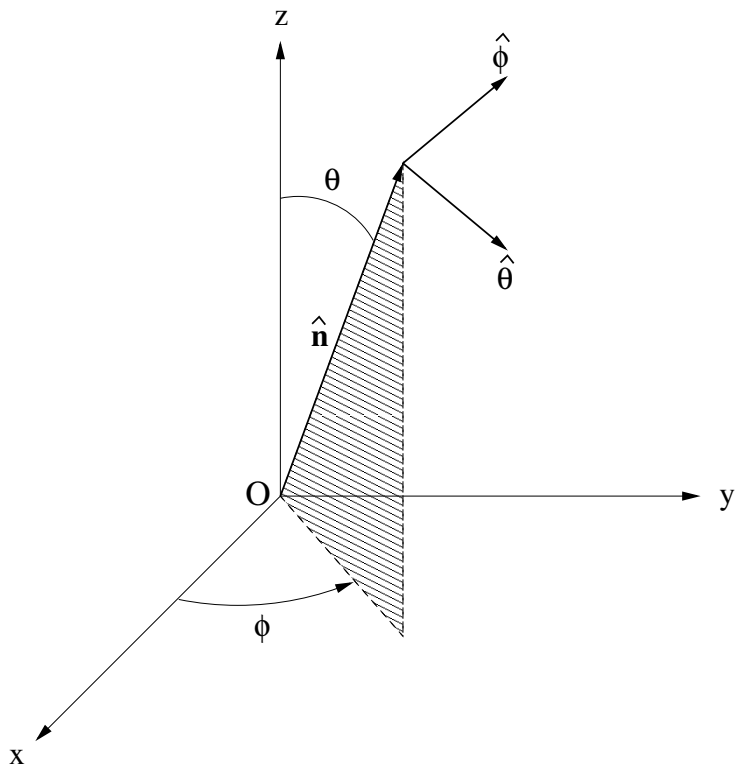

Figure 1: Coordinate system to describe the direction of propagation and the polarization state of a plane electromagnetic wave (adapted from Mishchenko).

The Stokes parameters are defined as follows:

$$I = \tfrac{1}{2}\sqrt{\tfrac{\varepsilon}{\mu}}(E_\theta E_\theta^* + E_\phi E_\phi^*), \tag{32}$$

$$Q = \tfrac{1}{2}\sqrt{\tfrac{\varepsilon}{\mu}}(E_\theta E_\theta^* - E_\phi E_\phi^*), \tag{33}$$

$$U = -\tfrac{1}{2}\sqrt{\tfrac{\varepsilon}{\mu}}(E_\theta E_\phi^* + E_\phi E_\theta^*), \tag{34}$$

$$V = i\tfrac{1}{2}\sqrt{\tfrac{\varepsilon}{\mu}}(E_\phi E_\theta^* - E_\theta E_\phi^*). \tag{35}$$

They are commonly defined as a 4×1 column vector $\mathbf{I}$ which is known as the Stokes vector (Chandrasekhar, 1950; Mishchenko et al., 2002). Since the Stokes parameters are real-valued and have the dimension of intensity, they can be measured directly with suitable instruments. The Stokes parameters are a complete set of quantities needed to characterize a plane electromagnetic wave. They carry information of the complex amplitudes and the phase difference. The first Stokes parameter I is the intensity and the other components Q, U, and V describe the polarization state of the wave. The Stokes parameters of a plane monochromatic wave are related by the quadratic identity

$$I^2 = Q^2 + U^2 + V^2. \tag{36}$$

The definition of a monochromatic plane wave implies that the complex amplitude $\mathbf{E_0}$ and the phase differences are constant. In the case of natural radiation the amplitudes and phases fluctuate, since the radiation originates from several sources that do not emit radiation coherently, and since the emission from one source usually has very short coherence times. This means that we usually have a superposition of radiation from several incoherent sources, and that the polarization state of the radiation from each source fluctuates as well. Such fluctuations have time scales that are longer than the period $(2\pi/\omega)$ of the oscillation, but that are still shorter than the integration time of the instrument that measures the radiation. Thus, the instrument measures an incoherent superposition of time averages over the fluctuating polarization. If the fluctuations are not completely random, the radiation is called partially polarized.

Since the different sources and/or emission events are assumed to be incoherent, the Stokes parameters can simply be added up:

$$I = \sum_i I_i\,,\ Q = \sum_i Q_i\,,\ U = \sum_i U_i\,,\ V = \sum_i V_i. \tag{37}$$

The equality Eq. (36) still holds for each contribution i, but for the resulting I,Q,U,V, we have in general the inequality

$$I^2 \geq Q^2 + U^2 + V^2. \tag{38}$$

The degree of polarization p is defined as

$$p = \frac{\sqrt{Q^2+U^2+V^2}}{I}. \tag{39}$$

For completely polarized radiation, $Q^2+U^2+V^2 = I^2$, thus $p = 1$, and for unpolarized radiation, $Q = U = V = 0$, thus $p = 0$.

In addition to the degree of polarization, p, the degree of linear polarization is defined as

$$p_{lin} = \frac{\sqrt{Q^2+U^2}}{I}, \tag{40}$$

and the the degree of circular polarization is defined as

$$p_{circ} = \frac{V}{I}. \tag{41}$$

2.2 Amplitude matrix

For the derivation of a relation between the incident and the scattered electric field we consider a finite scattering object in the form of a single body or a fixed aggregate embedded in an infinite homogeneous, isotropic and non-absorbing medium. We assume that the individual bodies forming the scattering object are sufficiently large that they can be characterized by optical constants appropriate to bulk matter, not to optical constants appropriate for single atoms or molecules. Solving the Maxwell equations for the internal volume, which is the interior of

the scattering object, and the external volume one can derive a formula, which expresses the total electric field everywhere in space in terms of the incident field and the field inside the scattering object. Applying the far field approximation gives a relation between incident and scattered field, which is that of a spherical wave. The amplitude matrix $\mathbf{S}(\hat{\mathbf{n}}^{\mathbf{sca}}, \hat{\mathbf{n}}^{\mathbf{inc}})$ includes this relation:

$$\begin{bmatrix} E_{\theta}^{sca}(r\hat{\mathbf{n}}^{\mathbf{sca}}) \\ E_{\phi}^{sca}(r\hat{\mathbf{n}}^{\mathbf{sca}}) \end{bmatrix} = \frac{e^{ikr}}{r}\mathbf{S}(\hat{\mathbf{n}}^{\mathbf{sca}}, \hat{\mathbf{n}}^{\mathbf{inc}}) \begin{bmatrix} E_{0\theta}^{inc} \\ E_{0\phi}^{inc} \end{bmatrix}. \tag{42}$$

The amplitude matrix depends on the directions of incident $\hat{n}^{inc}$ and scattering $\hat{n}^{sca}$ as well as on size, morphology, composition, and orientation of the scattering object with respect to the coordinate system. The distance between the origin and the observation point is denoted by r and the wave number of the external volume is denoted by k.

The amplitude matrix provides a complete description of the scattering pattern in the far field zone. The amplitude matrix explicitly depends on ϕ^{inc} and ϕ^{sca} even when θ^{inc} and/or θ^{sca} equal 0 or π.

2.3 Phase matrix

The phase matrix $\mathbf{P}$ describes the transformation of the Stokes vector of the incident wave into that of the scattered wave,

$$\mathbf{I}^{\mathbf{sca}}(r\hat{\mathbf{n}}^{\mathbf{sca}}) = \frac{1}{r^2}\mathbf{P}(\hat{\mathbf{n}}^{\mathbf{sca}}, \hat{\mathbf{n}}^{\mathbf{inc}})\mathbf{I}^{\mathbf{inc}}. \tag{43}$$

The 4×4 phase matrix can be written in terms of the amplitude matrix elements for single particles (Mishchenko et al., 2002). All elements of the phase matrix have the dimension of area and are real. As the amplitude matrix, the phase matrix depends on ϕ^{inc} and ϕ^{sca} even when θ^{inc} and/or θ^{sca} equal 0 or π. In general, all 16 elements of the phase matrix are non-zero, but they can be expressed in terms of only seven independent real numbers. Four elements result from the moduli $|S_{ij}|$ $(i, j = 1,2)$ and three from the phase-differences between S_{ij}. The non-zero degree of polarization Eq. (39) can be written in terms of the phase matrix elements

$$p = \frac{\sqrt{P_{21}^2 + P_{31}^2 + P_{41}^2}}{P_{11}}. \tag{44}$$

For spherical particles the phase matrix has only four independent elements that can be calculated from Mie-Theory (van de Hulst, 1981):

$$\mathbf{P}(\Theta) = \begin{bmatrix} P_{11}(\Theta) & P_{12}(\Theta) & 0 & 0 \\ P_{12}(\Theta) & P_{11}(\Theta) & 0 & 0 \\ 0 & 0 & P_{33}(\Theta) & P_{34}(\Theta) \\ 0 & 0 & -P_{34}(\Theta) & P_{33}(\Theta) \end{bmatrix} \tag{45}$$

In this case $\mathbf{P}$ depends only on the scattering angle Θ, which is obvious for symmetry reasons.

For randomly oriented, rotationally symmetric particles, six elements are required that also depend only on Θ:

$$\mathbf{P}(\Theta) = \begin{bmatrix} P_{11}(\Theta) & P_{12}(\Theta) & 0 & 0 \\ P_{12}(\Theta) & P_{22}(\Theta) & 0 & 0 \\ 0 & 0 & P_{33}(\Theta) & P_{34}(\Theta) \\ 0 & 0 & -P_{34}(\Theta) & P_{44}(\Theta) \end{bmatrix} \tag{46}$$

The phase matrices for rotationally symmetric particles can be calculated using the T-matrix method for moderate size parameters (Mishchenko et al., 2002).

In general, if there are several particles types which are not randomly oriented and have arbitrary shapes all 16 elements of the phase matrix can be independent. All elements depend on incoming and scattered direction, i.e. four angles.

2.4 Extinction matrix

In the special case of the exact forward direction ($\hat{\mathbf{n}}^{\mathbf{sca}} = \hat{\mathbf{n}}^{\mathbf{inc}}$) the attenuation of the incoming radiation is described by the extinction matrix $\mathbf{K}$. In terms of the Stokes vector we get

$$\mathbf{I}(r\hat{\mathbf{n}}^{\mathbf{inc}})\Delta S = \mathbf{I}^{\mathbf{inc}}\Delta S - \mathbf{K}(\hat{\mathbf{n}}^{\mathbf{inc}})\mathbf{I}^{\mathbf{inc}} + O(r^{-2}). \tag{47}$$

Here ΔS is a surface element normal to $\hat{\mathbf{n}}^{\mathbf{inc}}$. The extinction matrix can also be expressed explicitly in terms of the amplitude matrix. It has only seven independent elements. Again the elements depend on ϕ^{inc} and ϕ^{sca} even when the incident wave propagates along the z-axis.

For randomly oriented particles the extinction matrix is diagonal and does not depend on direction:

$$\mathbf{K} = \begin{bmatrix} C_{ext} & 0 & 0 & 0 \\ 0 & C_{ext} & 0 & 0 \\ 0 & 0 & C_{ext} & 0 \\ 0 & 0 & 0 & C_{ext} \end{bmatrix} \tag{48}$$

Here C_{ext} is the extinction cross section (see also Eq. 53).

2.5 Stokes emission vector

The particle also emits radiation if its temperature T is above zero Kelvin. According to Kirchhoff's law of radiation the emissivity equals the absorptivity of a medium under thermodynamic equilibrium. The energetic and polarization characteristics of the emitted radiation are described by a four-component Stokes emission column vector $\mathbf{a}(\hat{\mathbf{r}}, T, \omega)$. The emission vector is defined in such a way that the net rate, at which the emitted energy crosses a surface element ΔS normal to $\hat{\mathbf{r}}$ at distance r from the particle at frequencies from ω to $\omega + \Delta\omega$, is

$$W^e = \frac{1}{r^2}\mathbf{a}(\hat{\mathbf{r}}, T, \omega)B(T, \omega)\Delta S\Delta\omega, \tag{49}$$

where W^e is the power of the emitted radiation and B is the Planck function. In order to calculate $\mathbf{a}$ we assume that the particle is placed inside an opaque cavity of dimensions large compared to the particle and any wavelengths under consideration. We have thermodynamic equilibrium if the cavity and the particle are maintained at the constant temperature T. The emitted radiation inside the cavity is isotropic, homogeneous, and unpolarized. We can represent this radiation as a collection of quasi-monochromatic, unpolarized, incoherent beams propagating in all directions characterized by the Planck blackbody radiation

$$B(T,\omega)\Delta S\Delta\Omega = \frac{\hbar\omega^3}{2\pi^2c^2\left[\exp\left(\frac{\hbar\omega}{k_BT}\right)-1\right]}\Delta S\Delta\Omega, \tag{50}$$

where $\Delta\Omega$ is a small solid angle about any direction, $\hbar$ is the Planck constant divided by 2π, and k_B is the Boltzmann constant. The blackbody Stokes vector is

$$\mathbf{I_b}(T,\omega) = \begin{bmatrix} B(T,\omega) \\ 0 \\ 0 \\ 0 \end{bmatrix}. \tag{51}$$

For the Stokes emission vector we can derive

$$a_i^p(\hat{\mathbf{r}},T,\omega) = K_{i1}(\hat{\mathbf{r}},\omega) - \int_{4\pi} \mathrm{d}\hat{\mathbf{r}}' P_{i1}(\hat{\mathbf{r}},\hat{\mathbf{r}}',\omega), \quad i = 1\cdots 4. \tag{52}$$

This relation is a property of the particle only, and it is valid for any particle, in thermodynamic equilibrium or non-equilibrium.

For randomly oriented particles only the first element of the Stokes emission vector is non-zero and corresponds to the absorption cross section.

2.6 Optical cross sections

The optical cross-sections are defined as follows: The product of the scattering cross section C_{sca} and the incident monochromatic energy flux gives the total monochromatic power removed from the incident wave as a result of scattering into all directions. The product of the absorption cross section C_{abs} and the incident monochromatic energy flux gives the power which is removed from the incident wave by absorption. The extinction cross section C_{ext} is the sum of scattering and absorption cross section. One can express the extinction cross sections in terms of extinction matrix elements

$$C_{ext} = \frac{1}{I^{inc}}[K_{11}(\hat{\mathbf{n}}^{\mathbf{inc}})I^{inc} + K_{12}(\hat{\mathbf{n}}^{\mathbf{inc}})Q^{inc} + K_{13}(\hat{\mathbf{n}}^{\mathbf{inc}})U^{inc} + K_{14}(\hat{\mathbf{n}}^{\mathbf{inc}})V^{inc}], \tag{53}$$

and the scattering cross section in terms of phase matrix elements

$$\begin{aligned} C_{sca} = \frac{1}{I^{inc}}\int_{4\pi} \mathrm{d}\hat{\mathbf{n}}^{\mathbf{sca}}[&P_{11}(\hat{\mathbf{n}}^{\mathbf{sca}},\hat{\mathbf{n}}^{\mathbf{inc}})I^{inc} + P_{12}(\hat{\mathbf{n}}^{\mathbf{sca}},\hat{\mathbf{n}}^{\mathbf{inc}})Q^{inc} + \\ &P_{13}(\hat{\mathbf{n}}^{\mathbf{sca}},\hat{\mathbf{n}}^{\mathbf{inc}})U^{inc} + P_{14}(\hat{\mathbf{n}}^{\mathbf{sca}},\hat{\mathbf{n}}^{\mathbf{inc}})V^{inc}] \end{aligned} \tag{54}$$

The absorption cross section is the difference between extinction and scattering cross section:

$$C_{abs} = C_{ext} - C_{sca}. \tag{55}$$

The single scattering albedo ω_0, which is a commonly used quantity in radiative transfer theory, is defined as the ratio of the scattering and the extinction cross section:

$$\omega_0 = \frac{C_{sca}}{C_{ext}} \leq 1. \tag{56}$$

All cross sections are real-valued positive quantities and have the dimension of area.

The phase function is generally defined as

$$p(\hat{\mathbf{n}}^{\mathbf{sca}}, \hat{\mathbf{n}}^{\mathbf{inc}}) = \frac{4\pi}{C_{sca} I^{inc}} [P_{11}(\hat{\mathbf{n}}^{\mathbf{sca}}, \hat{\mathbf{n}}^{\mathbf{inc}}) I^{inc} + P_{12}(\hat{\mathbf{n}}^{\mathbf{sca}}, \hat{\mathbf{n}}^{\mathbf{inc}}) Q^{inc} + P_{13}(\hat{\mathbf{n}}^{\mathbf{sca}}, \hat{\mathbf{n}}^{\mathbf{inc}}) U^{inc} + P_{14}(\hat{\mathbf{n}}^{\mathbf{sca}}, \hat{\mathbf{n}}^{\mathbf{inc}}) V^{inc}] \tag{57}$$

The phase function is dimensionless and normalized:

$$\frac{1}{4\pi} \int_{4\pi} p(\hat{\mathbf{n}}^{\mathbf{sca}}, \hat{\mathbf{n}}^{\mathbf{inc}}) \mathrm{d}\hat{\mathbf{n}}^{\mathbf{sca}} = 1. \tag{58}$$

2.7 Vector radiative transfer equation

The vector radiative transfer equation can be derived from the Maxwell equations (Mishchenko et al., 2006):

$$\frac{\mathrm{d}\mathbf{I}}{\mathrm{d}s}(\mathbf{n}, \lambda) = -\langle \mathbf{K}(\mathbf{n}, \lambda) \rangle \mathbf{I}(\mathbf{n}, \lambda) + \langle \mathbf{a}(\mathbf{n}, \lambda) \rangle B(\lambda, T) + \int_{4\pi} \mathrm{d}\mathbf{n}' \langle \mathbf{Z}(\mathbf{n}, \mathbf{n}', \lambda) \rangle \mathbf{I}(\mathbf{n}', \lambda), \tag{59}$$

where $\mathbf{I}$ is the Stokes vector, $\langle \mathbf{K} \rangle$ is the ensemble-averaged extinction matrix, $\langle \mathbf{a} \rangle$ is the ensemble-averaged Stokes emission vector, B is the Planck function and $\langle \mathbf{Z} \rangle$ is the ensemble-averaged phase matrix. Moreover λ is the wavelength of the radiation, T is the temperature, $\mathrm{d}s$ is a path-length-element of the propagation path and $\mathbf{n}$ the propagation direction. Eq. (59) is valid for monochromatic or quasi-monochromatic radiative transfer.

It is important to note that $\langle \mathbf{Z} \rangle$ is here not the phase matrix in the particle frame but in the reference frame for the model atmosphere. For spherical or randomly oriented particles we may calculate the phase matrix $\langle \mathbf{P} \rangle$ as a function of the scattering angle only. $\langle \mathbf{Z} \rangle$ can be calculated as follows:

$$\langle \mathbf{Z} \rangle = \mathbf{L}(-\sigma_2) \langle \mathbf{P} \rangle \mathbf{L}(\pi - \sigma_1) \tag{60}$$

where $\mathbf{L}$ is the Stokes rotation matrix.

$$\mathbf{L}(\alpha) = \begin{bmatrix} 1 & 0 & 0 & 0 \\ 0 & \cos(2\alpha) & -\sin(2\alpha) & 0 \\ 0 & \sin(2\alpha) & \cos(2\alpha) & 0 \\ 0 & 0 & 0 & 1 \end{bmatrix} \tag{61}$$

The angles σ_1 and σ_2 can be calculated from the incident and scattered directions using spherical trigonometry (for details refer to Mishchenko et al. (2002)):

$$\cos\sigma_1 = \frac{\cos\theta^{sca} - \cos\theta^{inc}\cos\Theta}{\sin\theta^{inc}\sin\Theta} \tag{62}$$

$$\cos\sigma_2 = \frac{\cos\theta^{inc} - \cos\theta^{sca}\cos\Theta}{\sin\theta^{sca}\sin\Theta} \tag{63}$$

where

$$\begin{aligned}\Theta &= \arccos(\hat{\mathbf{n}}^{\mathbf{inc}}\cdot\hat{\mathbf{n}}^{\mathbf{sca}}) \\ &= \arccos(\cos\theta^{sca}\cos\theta^{inc} + \sin\theta^{sca}\sin\theta^{inc}\cos(\phi^{sca}-\phi^{inc}))\end{aligned} \tag{64}$$

is the scattering angle.

3 Surface Bidirectional Reflection Distribution Functions

The surface BRDF (Bidirectional Reflection Distribution Function) describes the distribution of scattered radiance from the surface. Basic reasons for the anisotropy of surface scattering are specular scattering (sun glint), rough surfaces, volumetric scattering, and geometric optical surface scattering, see Fig. 2. The surface BRDF and albedo are key parameter for climate simulations and remote sensing applications.

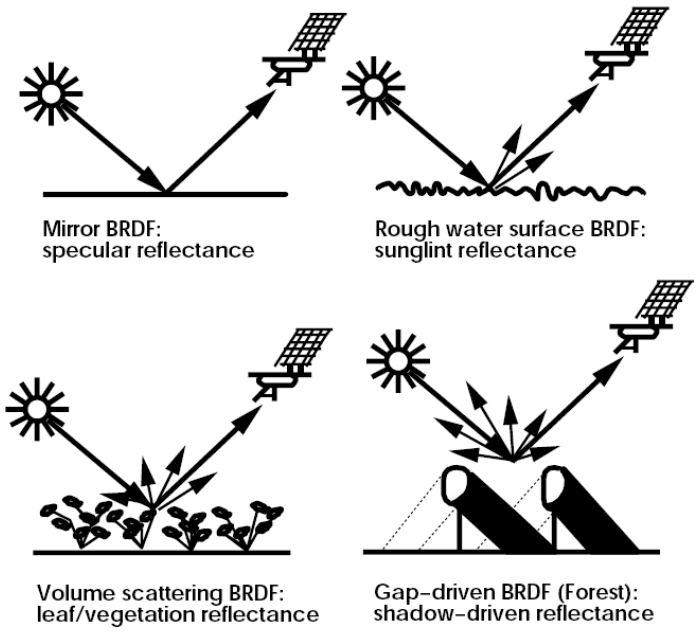

Figure 2: Basic reasons for the anisotropy of surface scattering (from MODIS BRDF/Albedo Product ATBD Version 5).

The BRDF R is defined as the ratio of reflected radiance per unit of incoming irradiance (Marshak and Davis, 2005), (Roberts, 2001)

$$R(\theta_i,\Phi_i,\theta_r,\Phi_r,\lambda,P) = \frac{I(\theta_r,\Phi_r)}{\mu_i F_i}. \tag{65}$$

where (θ_i,Φ_i) and (θ_r,Φ_r) is the direction of the incoming and of the reflected radiance respectively, F_i is the incoming flux, μ_i is the cosine of the associated zenith angle, and P the wave polarization. The BRDF provides the lower boundary condition for the solution of the radiative transfer Eq. (14).
In order to be physically realistic, the BRDF must fulfill at least the Helmholtz Reciprocity

$$R(\theta_i,\Phi_i,\theta_r,\Phi_r) = R(\theta_r,\Phi_r,\theta_i,\Phi_i) \tag{66}$$

and energy conservation

$$\int_0^{2\pi} d\Phi_r \int_0^{\pi/2} d\theta_r R(\theta_i,\Phi_i,\theta_r,\Phi_r,\lambda)\sin(\theta_r)\cos(\theta_r) \leq 1. \tag{67}$$

3.1 Physically based BRDF model

Physically based models are the most complex BRDF models compared to semi-empirical and empirical models. They deal with the underlying physics in an exact way. Physical models aim for describing the geometric shapes of the vegetation (geometric models), treat canopies as a volumes of scattering and absorbing particles (turbid medium models), or even intend to describe them by crowds of individual vegetation elements (complex models). A recent intercomparison of three-dimensional complex models is performed at the *RAdiation transfer Model Intercomparison* (RAMI) (Pinty et al., 2004). During the intercomparison the RAMI On-line Model Checker (ROMC) (Widlowski et al., 2008) was developed, that allows to check the performance of vegetation resolving radiative transfer models. Some of the RAMI scenarios are illustrated in Fig. 3.

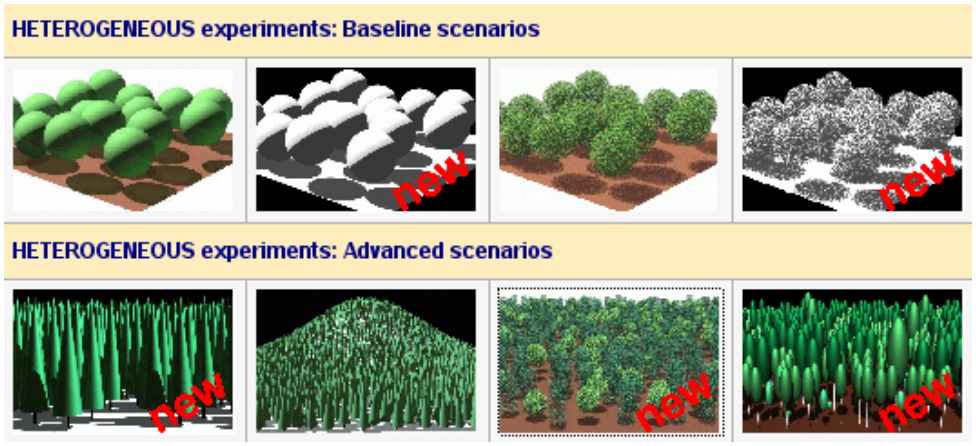

Figure 3: Heterogeneous scenarios examined in the RAMI intercomparison (from the RAMI web page).

Linear Kernel-based BRDF models have the general form

$$R(\theta_i,\Phi_i,\theta_r,\Phi_r,\lambda) = \sum_k f_k(\lambda) K_k(\theta_i,\theta_r,\Phi), \tag{68}$$

where K_k are the Kernels, representing the directional distribution of the scattered light, f_k are spectrally dependent parameters derived from measurements, and $\Phi = \Phi_i - \Phi_r$ is the relative azimuth of the reflection event. Following (Roujean et al., 1992) most of the recent models use a three Kernel structure:

$$R(\theta_i,\Phi_i,\theta_r,\Phi_r,\lambda) = f_{iso}(\lambda) + f_{vol}(\lambda) K_{vol}(\theta_i,\theta_r,\Phi) + f_{geo}(\lambda) K_{geo}(\theta_i,\theta_r,\Phi). \tag{69}$$

For the *Ross-Thick* volume scattering Kernel K_{vol}, there is general agreement between the models

$$K_{vol}(\theta_i,\theta_r,\Phi) = \frac{4}{3\pi}\frac{1}{\cos(\theta_i)+\cos(\theta_r)}\left[\left(\frac{\pi}{2}-\zeta\right)\cos\zeta + \sin\zeta\right] - \frac{1}{3}, \tag{70}$$

where ζ is the phase angle of scattering defined as

$$\zeta = \cos^{-1}(\cos\theta_i \cos\theta_r + \sin\theta_i \sin\theta_r \cos\Phi). \tag{71}$$

But the *geometric-optical* Kernel K_{geo} is still under discussion. The *Roujean* model (Roujean et al., 1992) uses following expression

$$\begin{aligned} K_{geo}(\theta_i, \theta_r, \Phi) &= \frac{1}{2\pi}[(\pi - \Phi)\cos\Phi + \sin\Phi]\tan\theta_i \tan\theta_r \\ &\quad - \frac{1}{\pi}\left[\tan\theta_i + \tan\theta_r + \sqrt{\tan^2\theta_i + \tan^2\theta_r + 2\tan\theta_i \tan\theta_r \cos\Phi}\right]. \end{aligned} \tag{72}$$

The *non-reciprocal Li-Sparse (LS)* model (Li and H.Strahler, 1992; Li et al., 1996) is designed for simulation of sparse vegetation covers like grass, shrub lands, emerging crops or bare soil surfaces. It uses following geometric Kernel:

$$K_{geo}(\theta_i, \theta_r, \Phi) = \frac{1}{\pi}(t - \sin t \cos t)(\sec\theta_i + \sec\theta_r) - (\sec\theta_i + \sec\theta_r) + \frac{1}{2}(1 + \cos\zeta)\sec\theta_r, \tag{73}$$

where

$$\cos t = \frac{\sqrt{D^2 + (\tan\theta_i \tan\theta_r \cos\Phi)^2}}{(\sec\theta_i + \sec\theta_r)} \tag{74}$$

and

$$D = \sqrt{\tan^2\theta_i + \tan^2\theta_r - 2\tan\theta_i \tan\theta_r \cos\Phi}. \tag{75}$$

The *reciprocal Li-Sparse (LSR)* model is a slight modified version of the LS model, which satisfy the Helmholtz reciprocity Eq. (66)

$$K_{geo}(\theta_i, \theta_r, \Phi) = \frac{1}{\pi}(t - \sin t \cos t)(\sec\theta_i + \sec\theta_r) - (\sec\theta_i + \sec\theta_r) + \frac{1}{2}(1 + \cos\zeta)\sec\theta_i \sec\theta_r. \tag{76}$$

The *Li-Dense* model is primarily designed for simulating dense canopies of high reaching vegetation covers. It uses following geometric Kernel:

$$K_{geo}(\theta_i, \theta_r, \Phi) = \frac{1 + \cos\zeta \sec\theta_r}{\cos\theta_i + \cos\theta_r - (t - \sin t \cos t)(\sec\theta_i + \sec\theta_r)/\pi} - 2. \tag{77}$$

The *RPV* model (Rahman et al., 1993) is a semi-empirical multiplicative BRDF model. It is able to describe the BRDF of arbitrary natural surfaces, ranging from bare soil to canopy covers. The model expresses surface anisotropy using three terms: ρ_0 characterizes the intensity of the reflectance, k describes the surface anisotropy and Θ controls the relative amount of forward and backward scattering.

$$R(\theta_i, \Phi_i, \theta_r, \Phi_r, \lambda) = \rho_0 \frac{\cos^{k-1}\theta_i \cos^{k-1}\theta_r}{(\cos\theta_i + \cos\theta_r)^{1-k}} F(g)[1 + R(G)], \tag{78}$$

where $F(g)$ describes the forward/backward scattering

$$F(g) = \frac{1-\Theta^2}{[1+\Theta^2-2\Theta\cos(\pi-g)]^{1.5}}, \tag{79}$$

The phase angle g is given by

$$\cos g = \cos\theta_i \cos\theta_r + \sin\theta_i \sin\theta_r \cos(\Phi_i - \Phi_r) \tag{80}$$

The hot spot effect is expressed by

$$1 + R(G) = 1 + \frac{1-\rho_0}{1+G} \tag{81}$$

and the geometric factor G is given by

$$G = [\tan^2\theta_i + \tan^2\theta_r - 2\tan\theta_i \tan\theta_r \cos(\Phi_i - \Phi_r)]^{1/2}. \tag{82}$$

The RPV model was modified by Martonchik (Martonchik, 1997) into a nearly linear form.

3.2 Empirical models

Empirical BRDF models are created with the intention to fit a function to the data to describe the surface BRDF. Advantages of empirical models lie in the simplicity and the lack of assumptions made about the surface type, but there is a deficit of physical meaning of the parameters.
As empirical models do not perform as well as physical model, we concentrate here only on the commonly used Walthall model (Walthall et al., 1985), which express the BRDF in the following format:

$$R = f_0 + f_1\theta_r^2 + f_2\theta_r\cos(\Phi_r - \Phi_i), \tag{83}$$

where f_0, f_1 and f_2 are coefficients derived through least square fits. The disadvantage of the Walthall model is that is does not fulfill the Helmholtz reciprocity Eq. (66). The modified Walthall model (Nilson and Kuusk, 1989) (Walthall et al., 1985) fixes this shortcoming

$$R = f_0 + f_1(\theta_r^2 + \theta_i^2) + f_2(\theta_r^2\theta_i^2) + f_3\theta_r\theta_i\cos(\Phi_r - \Phi_i). \tag{84}$$

3.3 Calculating the Albedo from BRDF models

In order to calculate the albedo, the BRDF is integrated over all angles of the reflected radiation. The albedo is dependent on the illumination of the scene. For directional illumination the albedo, black sky albedo A_{BS}, is defined as follows:

$$A_{BS}(\theta_i) = \int_0^{2\pi} d\Phi_r \int_0^{\pi/2} d\theta_r R(\theta_i, \Phi_i, \theta_r, \Phi_r, \lambda)\sin(\theta_r)\cos(\theta_r). \tag{85}$$

For diffuse illumination the albedo is called white sky albedo A_{WS} and is defined by:

$$A_{WS} = \frac{1}{\pi}\int_0^{\pi/2} d\theta_i \int_0^{2\pi} d\Phi_i \int_0^{\pi/2} d\theta_r \int_0^{2\pi} d\Phi_r R(\theta_i, \Phi_i, \theta_r, \Phi_r, \lambda)\sin(\theta_i)\cos(\theta_i)\sin(\theta_r)\cos(\theta_r).$$

(86)

For Kernel-based BRDFs the integration can be performed directly on the Kernel. The directional hemispherical and bihemispherical integrals of the BRDF models Kernels are defined as

$$h_k(\theta_i) = \int_0^{2\pi} d\Phi \int_0^{\pi/2} d\theta_r K_k(\theta_i, \theta_r, \Phi) \sin(\theta_r) \cos(\theta_r) \tag{87}$$

and

$$H_k = 2 \int_0^{\pi/2} d\theta_i h_k(\theta_i) \sin(\theta_i) \cos(\theta_i) \tag{88}$$

Hence the white sky albedo and the black sky albedo are

$$A_{BS}(\theta_i) = \sum_k f_k h_k(\theta_i) \tag{89}$$

and

$$A_{WS} = \sum_k f_k H_k \tag{90}$$

It is worthwhile to note, that in case of the Kernel based BRDF the directional integration can be performed for each Kernel in advance, independently of the individual simulation.

References

Chance, K. and Spurr, R. J. D.: Ring effect studies: Rayleigh scattering including molecular parameters for rotational Raman scattering, and the Fraunhofer spectrum, Appl. Opt., 36, 5224–5230, 1997.

Chandrasekhar, S.: Radiative transfer, Oxford Univ. Press, UK, 1950.

Dahlback, A. and Stamnes, K.: A new spherical model for computing the radiation field available for photolysis and heating at twilight, Planet. Space Sci., 39, 671–683, 1991.

Emde, C.: A Polarized Discrete Ordinate Scatterig Model for Radiative Transfer Simulations in Spherical Atmospheres with Thermal Source, Ph.D. thesis, University of Bremen, ISBN 3-8325-0885-4, 2005.

Emde, C. and Kylling, A.: Development plan for libRadtran demonstration version, Tech. Rep. ESTEC Contract No AO/1-5433/07/NL/HE, Deutsches Zentrum für Luft- und Raumfahrt, Wessling, Germany, 2008.

Emde, C. and Mayer, B.: Simulation of solar radiation during a total solar eclipse: A challenge for radiative transfer, Atmos. Chem. Phys., 7, 2259–2270, 2007.

Evans, K. F. and Stephens, G. L.: A new polarized atmospheric radiative transfer model, J. Quant. Spectrosc. Radiat. Transfer, 46, 413–423, 1991.

Jackson, J. D.: Classical Electrodynamics, John Wiley & Sons, New York, 1975.

Joiner, J., Bhartia, P. K., Cebula, R. P., Hilsenrath, E., McPeters, R. D., and Park, H.: Rotational Raman scattering (Ring effect) in satellite backscatter ultraviolet measurements, Appl. Opt., 21, 4513–4525, 1995.

Kattawar, G. W., Young, A. T., and Humphreys, T. J.: Inelastic scattering in planetary atmospheres. I. The Ring effect, without aerosols, The Astrophysical Journal, 243, 1049–1057, 1981.

Kylling, A. and Stamnes, K.: Efficient yet accurate solution of the linear transport equation in the presence of internal sources: the exponential–linear–in–depth approximation, J. Com. Phys., 102, 265–276, 1992.

Landgraf, J., Hasekamp, O. P., van Deelen, R., and Aben, I.: Rotational Raman scattering of polarized light in the Earth atmosphere: a vector radiative transfer model using the radiative transfer perturbation theory approach, J. Quant. Spectrosc. Radiat. Transfer, 87, 399–433, 2004.

Li, X. and H.Strahler, A.: Geometric-optical bi-directional reflectance modeling of the discrete crown vegetation canopy: effect of crown shape and mutual shadowing, IEEE Transactions on Geoscience and Remote Sensing, 30, 276–292, 1992.

Li, Z., Cihlar, J., Zheng, X., Morceau, L., and Ly, H.: The bidirectional effects of AVHRR measurements over Boreal regions, IEEE Transactions on Geoscience and Remote Sensing, 34, 1308–1322, 1996.

Marshak, A. and Davis, A.: 3D Radiative Transfer in Cloudy Atmospheres, Springer, iSBN-13 978-3-540-23958-1, 2005.

Martonchik, J. V.: Determination of aerosol optical depth and land surface directional reflectance using multi-angle imagery, J. Geophys. Res., 102, 17 015–17 022, 1997.

Mayer, B.: I3RC phase 1/2 results from the MYSTIC Monte Carlo model, in: Intercomparison of three-dimensional radiation codes: Abstracts of the first and second international workshops, edited by Cahalan, R. and Davis, R., pp. 49–54/107–108, Institute of Atmospheric Physics, University of Arizona, iSBN 0-9709609-0-5, 2000.

Mishchenko, M. I., Travis, L., and Lacis, A.: Scattering, Absorption, and Emission of Light by Small Particles, Cambridge University Press, 2002.

Mishchenko, M. I., Travis, L. D., and Lacis, A. A.: Multiple Scattering of Light by Particles: Radiative Transfer and Coherent Backscattering, Cambridge University Press, 2006.

Nilson, T. and Kuusk, A.: A reflectance model for the homogeneous plant canopy and its inversion, Remote Sens. Environ., 66, 157–167, 1989.

Pinty, B., Widlowski, J.-L., Taberner, M., Gobron, N., Verstraete, M. M., Disney, M., Gascon, F., Gastellu, J.-P., Jiang, L., Kuusk, A., Lewis, P., Li, X., Ni-Meister, W., Nilson, T., North, P., Qin, W., Su, L., Tang, S., Thompson, R., Verhoef, W., Wang, H., Wang, J., Yan, G., and Zang, H.: Radiation transfer model intercomparison (RAMI) exercise: Results from the second phase, J. Geophys. Res., 109, D06 210, doi:10.1029/2003JD004 252, 2004.

Rahman, H., Pinty, B., and Verstraete, M. M.: Coupled surface–atmosphere reflectance (CSAR) model 2. semiempirical surface model usable with NOAA advanced very high resolution radiometer data, J. Geophys. Res., 98, 20,791–20,801, 1993.

Roberts, G.: A review of the application of BRDF models to infer land cover parameters at regional and global scales, Progress in Physical Geography, 25, 483–511, 2001.

Roujean, J.-L., Leroy, M., and Deschamps, P.: A bidirectional reflectance model of the Earth's surface for the correction of remote sensing data, J. Geophys. Res., 97, 20 455–20 468, 1992.

Spurr, R., de Haan, J. D., van Oss, R., and Vasilkov, A.: Discrete ordinate radiative transfer in a stratified medium with first order rotational Raman scattering, J. Quant. Spectrosc. Radiat. Transfer, 109, 404–425, 2008.

Stamnes, K., Tsay, S.-C., Wiscombe, W., and Jayaweera, K.: Numerically stable algorithm for discrete–ordinate–method radiative transfer in multiple scattering and emitting layered media, Appl. Opt., 27, 2502–2509, 1988.

Stamnes, K., Tsay, S.-C., Wiscombe, W., and Laszlo, I.: DISORT, a General-Purpose Fortran Program for Discrete-Ordinate-Method Radiative Transfer in Scattering and Emitting Layered Media: Documentation of Methodology, Tech. rep., Dept. of Physics and Engineering Physics, Stevens Institute of Technology, Hoboken, NJ 07030, 2000.

van de Hulst, H. C.: Light Scattering by Small Particles, Dover, 1981.

Vountas, M., Rozanov, V. V., and Burrows, J. P.: Ring effect: impact of rotational Raman scattering on radiative transfer in Earht's atmosphere, J. Quant. Spectrosc. Radiat. Transfer, 60, 943–961, 1998.

Walthall, C., Norman, J., Welles, J., Campbell, G., and Blad, B.: Simple equation to approximate the bi-directional relectance from vegetation canopies and bare soil surfaces, Applied Optics, 24, 383–387, 1985.

Widlowski, J.-L., Robustelli, M., Disney, M., Gastellu-Etchegorry, J.-P., Lavergne, T., Lewis, P., North, P., Pinty, B., Thompson, R., and Verstraete, M.: The RAMI On-line Model Checker (ROMC): A web-based benchmarking facility for canopy reflectance models, Remote Sensing of Environment, 112, 1144–1150, doi:10.1016/j.rse.2007.07.016, 2008.

Young, A. T.: On the Rayleigh–scattering optical depth of the atmosphere, J. of Applied Meteorology, 20, 328–330, 1981a.

Young, A. T.: Rayleigh scattering, Appl. Opt, 20, 533–535, 1981b.